Identification and characterization of a new cognitive enhancer based on inhibition of insulin-regulated aminopeptidase

Anthony L. Albiston,* Craig J. Morton,§ Hooi Ling Ng,§ Vi Pham,* Holly R. Yeatman,* Siying Ye,*,1 Ruani N. Fernando,*,2 Dimitri De Bundel,*,3 David B. Ascher,§ Frederick A. O. Mendelsohn,* Michael W. Parker,†,§,4 and Siew Yeen Chai*,‡,4,5

*Howard Florey Institute, Florey Neurosciences Institutes, †Department of Biochemistry and Molecular Biology, Bio21 Molecular Science and Biotechnology Institute, and ‡Centre for Neuroscience, University of Melbourne, Parkville, Victoria, Australia; and §St. Vincent's Institute of Medical Research, Fitzroy, Victoria, Australia

ABSTRACT   Approximately one-quarter of people over the age of 65 are estimated to suffer some form of cognitive impairment, underscoring the need for effective cognitive-enhancing agents. Insulin-regulated aminopeptidase (IRAP) is potentially an innovative target for the development of cognitive enhancers, as its peptide inhibitors exhibit memory-enhancing effects in both normal and memory-impaired rodents. Using a homology model of the catalytic domain of IRAP and virtual screening, we have identified a class of nonpeptide, small-molecule inhibitors of IRAP. Structure-based computational development of an initial "hit" resulted in the identification of two divergent families of compounds. Subsequent medicinal chemistry performed on the highest affinity compound produced inhibitors with nanomolar affinities (K_i 20–700 nM) for IRAP. *In vivo* efficacy of one of these inhibitors was demonstrated in rats with an acute dose (1 nmol in 1 μl) administered into the lateral ventricles, improving performance in both spatial working and recognition memory paradigms. We have identified a family of specific IRAP inhibitors that is biologically active which will be useful both in understanding the physiological role of IRAP and potentially in the development of clinically useful cognitive enhancers. Notably, this study also provides unequivocal proof of principal that inhibition of IRAP results in memory enhancement.—Albiston, A. L., Morton, C. J., Ng, H. L., Pham, V., Yeatman, H. R., Ye, S., Ruani, N., Fernando, R. N., De Bundel, D., Ascher, D. B., Mendelsohn, F. A. O., Parker, M. W., Chai, S. Y. Identification and characterization of a new cognitive enhancer based on inhibition of insulin-regulated aminopeptidase. *FASEB J.* 22, 4209–4217 (2008)

Key Words: facilitation of memory · drug development · virtual screening · homology model · glucose uptake

COGNITIVE DECLINE, MOST COMMONLY associated with Alzheimer's dementia, can also result from other conditions, including cerebral ischemia or brain trauma. Most drugs under clinical development for the treatment of cognitive decline target the cholinergic system: The majority of U.S. Food and Drug Administration (FDA) approved drugs are cholinesterase inhibitors, and all demonstrate limited efficacy (1). The development of insulin-regulated aminopeptidase (IRAP; EC 3.4.11.3) inhibitors as drug candidates provides an alternative therapeutic class based on a novel target. Peptide inhibitors of IRAP, when administered centrally into the lateral ventricles, facilitate spatial and aversion-related memories in normal rodents (2–5). More importantly, these inhibitors restore memory in animals with memory deficits induced by alcohol (6), ischemia (7), perforant pathway lesions (4), or chemical perturbations of the septo-hippocampal cholinergic pathway (8–11). The mechanisms whereby IRAP inhibitors facilitate memory are not fully understood (12), but recent studies implicate the involvement of neuroendocrine mechanisms. Inhibition of IRAP may extend the half-life of neuropeptides that modify learning and memory processes (13). Peptide substrates of IRAP include arginine-vasopressin, oxytocin, met-enkephalin, somatostatin, dynorphin A$_{(1-8)}$, and lys-bradykinin, all of which are known to modulate memory (14, 15).

---

[1] Current address: Department of Physiology, Dartmouth Medical School, Hanover, NH, USA.

[2] Current address: Division of Molecular Neurobiology, Department of Medical Biochemistry and Biophysics, Karolinska Institute, Stockholm, Sweden.

[3] Current address: Research Group of Experimental Pharmacology, Department of Pharmaceutical Chemistry, Drug Analysis and Drug Information, Vrije University, Brussel, Brussels, Belgium.

[4] These authors contributed equally to this work.

[5] Correspondence: Howard Florey Institute, University of Melbourne, Parkville, VIC 3010, Australia. E-mail: sychai@florey.edu.au

IRAP was first identified in adipocytes, where it was found associated with the inducible glucose transporter GLUT4. The protein coexists with GLUT4 in specialized vesicles and accompanies it to the plasma membrane in response to insulin stimulation (16). In these insulin-responsive tissues, IRAP is proposed to play a role in the intracellular retention of GLUT4 vesicles (17). This protein was also cloned from a placental cDNA library as oxytocinase and is thought to be the principal enzyme involved in the regulation of circulating oxytocin levels during pregnancy (18). Most recently, it was demonstrated to be the specific binding site for the memory-enhancing peptides angiotensin IV (Ang IV) and LVV-hemorphin 7 (LVV-H7) (19).

In the brain, IRAP is found in high concentrations in regions involved in cognitive function, including the cerebral cortex, hippocampus, basal forebrain, and amygdala (20), where it is coexpressed with the glucose transporter GLUT4 in neurons. It was recently demonstrated that IRAP inhibitors increase activity-evoked glucose uptake into the pyramidal neurons of the hippocampus (21). Glucose is a potent modulator of learning and memory in both humans and rodents (22–24), with increases in glucose demand in the hippocampus occurring during memory processing (25).

To date, the only published IRAP inhibitors are the peptides Ang IV and LVV-H7 (19) and their modified forms (26–28). Although these peptides are high-affinity, competitive inhibitors of IRAP (14, 15), they display promiscuity at higher concentrations, binding to other proteins including aminopeptidase N (29, 30). This, together with the rapid onset of some of the physiological responses of these peptides, has led some investigators to propose that IRAP is not the protein involved in mediating the central effects of Ang IV and LVV-H7 (31). In addition to problems with selectivity, the peptide inhibitors have limited potential for development into clinically useful cognitive enhancers because of their other biochemical properties: susceptibility to degradation and lack of blood brain barrier permeability. In view of this, we have utilized a high-throughput computational docking approach (32, 33) to successfully identify new drug-like, nonpeptide inhibitors of IRAP.

MATERIALS AND METHODS

Generation of the homology model

The protease region of IRAP (residues L140 to S533) was modeled on the structure of the equivalent domain of another M1 aminopeptidase, leukotriene A4 hydrolase (LTA4H), (residues S8 to L389; PBD code 1HS6) (34). While the overall identity between the sequences is low, the region immediately surrounding the active site residues, including the HEXXH and GXMEN motifs, is relatively well conserved, with 41% sequence identity. A sequence alignment of the catalytic domains of several members of the M1 aminopeptidase family, including IRAP and LTA4H, was used to guide model building. The model was built using COMPOSER in Sybyl6.8 (Tripos Inc., St. Louis, MO, USA) and minimized in Sybyl6.8 under the Tripos Force Field, with the final structure having more than 95% of residues in the allowed region of a Ramachandran plot. A zinc ion was manually added to the active site motif after comparison with the zinc-bound LTA4H structure indicated the conformation of residues in the zinc-binding motif was identical in the two proteins. The quality of the model was confirmed with Verify3D (35) (data not shown). Model structures were examined using Sybyl6.8.

In silico screening

Virtual compound libraries were assembled from online databases of a number of commercial suppliers. Prior to screening, the libraries were refined to select only "drug-like" compounds using FILTER (OpenEye, Santa Fe, NM, USA) giving ~1.5 million structures, which were then converted to three-dimensional (3D) structures using Omega (OpenEye). Virtual screening was carried out with FRED (OpenEye) using the ShapeGauss scoring function. The 58 compounds with the highest docking scores were purchased and tested in an in vitro IRAP enzymatic assay. A 3D similarity search using ROCS (OpenEye) was conducted initially on HFI-14 (compound with the highest affinity for IRAP in the first round of screening) and later on HFI-142. Compounds with high shape complementarity (Tanimoto coefficient >0.85) were selected for in vitro assays. A 2D similarity search was also performed using Unity (Tripos, St. Louis, MO, USA). Approximately 200 compounds with high shape or 2D complementarity (Tanimoto coefficient >0.85) were selected for in vitro assays.

Synthesis of compounds

The 2-amino-4-aryl-4H-chromene-3-carboxylic acid esters, including HFI-142 and HFI-435, were prepared from the appropriate aromatic aldehyde and phenol using general reaction conditions described elsewhere (36).

Enzyme assays

IRAP

The enzymatic activity of IRAP (specific activity 10.6 U/mg) was determined by the hydrolysis of the synthetic substrate L-leucine 7-amido-4-methyl coumarin hydrochloride (Leu-MCA) (Sigma-Aldrich, St. Louis, MO, USA), monitored by the release of a fluorogenic product, MCA, at excitation and emission wavelengths of 380 and 440 nm, respectively, as described elsewhere (15). Initial screenings for inhibitors utilized membrane preparations from HEKT cells transfected with pCI-IRAP (a gift from Masafumi Tsujimoto, RIKEN, Saitama, Japan) (15), with subsequent analyses utilizing purified recombinant extracellular domain of IRAP obtained from insect cells (unpublished results).

LTA4H

Recombinant human LTA4H (Cayman Chemical, Ann Arbor, MI, USA) (specific activity 166 U/mg) was incubated at room temperature with 100 μM alanine-β-naphthylamide as substrate in 50 mM Tris-HCl buffer, pH 8.0, containing 100 mM KCl with or without increasing concentrations of an inhibitor. The fluorescence was measured at 320 nm excitation and 405 nm emission.

Aminopeptidase N

Aminopeptidase N (specific activity 40 U/mg) (Sigma Aldrich) was incubated with 250 µM of substrate alanine-β-naphthyl-amide (Sigma Aldrich) in Tris buffered saline (50 mM Tris-HCl, 150 mM NaCl pH 7.5) at 25°C. IRAP inhibitors (1–10 µM) were added after 1 min and fluorescence was monitored at 320 nm excitation and 405 nm emission.

Endoplasmic reticulum-associated aminopeptidases 1 and 2 (ERAP1 and ERAP2)

The enzymatic activities of purified recombinant soluble ERAP1 and ERAP2 (specific activities 2.1 and 18.0 U/mg, respectively; unpublished results) were determined by the hydrolysis of the synthetic substrates, Leu-MCA and Arg-MCA, respectively (Sigma-Aldrich), using the same methodology as used with recombinant IRAP. Briefly, 1–10 µg purified protein was incubated with the substrate (12.5 to 500 µM) and inhibitors (10 nM to 1 mM) in 25 mM Tris, pH 7.4, with 150 mM NaCl. Activity was measured at excitation 380 nm and emission 440 nm.

Angiotensin converting enzyme (ACE)

ACE (specific activity 10 U/mg) (Sigma Aldrich) was incubated with 5 mM hippuryl-histidyl leucine (HHL) in 100 mM potassium buffer (pH 8.3) that contained 300 mM NaCl and 100 µM $ZnSO_4$ for 30 min at 37°C. The enzymatic reaction was stopped by the addition of 0.28N NaOH, *o*-phthaldialdehyde (20 mg/ml) in methanol was added, and the fluorescent reaction stopped by the addition of 200 µl of 3N HCl. The product, L-HL, was measured fluorometrically at 360 nm excitation and 500 nm emission.

Determination of blood-brain barrier permeability

Compounds (5 mg/kg) dissolved in 1% (v/v) dimethyl sulfoxide (DMSO) were administered to male Swiss outbred mice intravenously. At various time points (5, 30, 60, and 240 min), the mice were anesthetized, and blood was obtained by cardiac puncture. Following cervical dislocation, the brain was removed, and both brain and plasma concentrations of compound were determined using liquid chromatography-mass spectrometry techniques. The amount of compound associated with the brain vasculature was subtracted (this was determined with a known brain vascular volume obtained following administration of the nonabsorbable marker ^{14}C-inulin) and the brain/plasma ratio was determined at each time point.

Surgical preparation of rats and drug treatment

All experiments were performed according to the National Health and Medical Research Council of Australia "Code of practice for the care and use of animals for scientific purposes." Male Sprague Dawley rats (250–270 g) were housed individually and given water and standard rat chow *ad libitum*. The rats were anesthetized with 5% (v/v) isofluorane and stereotaxically implanted with a chronic indwelling cannula (Plastics One, Roanoke, VA, USA) into the cerebral lateral ventricle using the following flat skull coordinates: 0.8 mm posterior to bregma, 1.5 mm lateral to midline, and 3.5 mm ventral to the dura (37). The cannula was then secured to the skull with stainless steel screws and dental cement. Seven days following surgery, correct cannula placement was verified by the dipsogenic response to angiotensin II (0.1 nmol in 2 µl). For all behavioral tests, the animals were habituated for at least 2 h in the testing room, injected with 0.1 or 1 nmol HFI-419 in 2 µl of 10% (v/v) DMSO

or vehicle and then returned to their home cage for 5 min prior to testing.

Novel object recognition task

Prior to the acquisition trial, the rats were habituated for 5 min in the testing box (made from gray Perspex of dimensions 60×60×50 cm) in diffuse dim light and then returned to their home cage (38). The rats were placed in the testing box facing away from 2 identical objects that had been secured to the floor in adjacent corners of the box. The rats were allowed 5 min to explore the objects, with exploration defined as the nose being less than 2 cm from the object when facing the object. On day 2 of testing, after an intertrial interval of 20 h, one of the objects was replaced by a novel object made from the same material but of a different shape, and the rats were given 2 min in the box. The recognition index was determined as the time spent exploring the novel object minus the time spent on the familiar object, divided by the time spent on both objects.

Spontaneous alternation plus maze

The plus maze was made of black plastic and composed of 4 arms, with each arm measuring $75 \times 10 \times 20$ cm and visual cues placed 1 m away from the maze. Spontaneous alternation testing was conducted by placing the rat in the center of the maze and allowing 20 min of unimpeded exploration (39). The number and sequence of arm entries were recorded for calculation of a percentage alternation score. An alternation consisted of 4 different arm choices over 5 consecutive arm entries. An alternation score was derived by dividing the number of observed alternations in overlapping quintuplets by the number of possible alternations.

Elevated plus maze

The maze consisted of 2 open arms (70×10 cm) with a 5-cm high surrounding wall and 2 enclosed arms (70×10 cm) with a 27-cm high surrounding wall. The floors were black laminate, the open arm walls were clear Perspex, and the closed arm walls black Perspex. The maze was elevated 85 cm above the ground. Rats were placed in the central platform facing one of the closed arms, and behavior was monitored for 10 min using Ethovision software (Noldus Information Technology, Wageningen, The Netherlands). The percentage of time spent in the open arms compared to the closed arms was a measure of the anxiety of the animals. The activity of each rat was video-recorded and scored automatically by the Ethovision software.

Locomotor cell activity

Locomotor activity of rats was monitored in cages measuring $40 \times 40 \times 40$ cm (Coulbourn Instruments, Whitehall, PA, USA) equipped with infrared photobeams for 30 min. Activity was measured when pairs of photobeams spaced 2.54 cm apart, providing a 1.27-cm spatial resolution, were crossed. Data were collected and analyzed using TruScan Photo Beam Activity system (Coulbourn Instruments).

Hippocampal glucose uptake assay

Male Sprague-Dawley rats (250–270 g) were anesthetized with Isofluorane and killed by decapitation. The brains were rapidly removed and placed into ice-cold, carbogen-bubbled, artificial cerebrospinal fluid (aCSF: 124 mM NaCl, 2.5 mM KCl, 2 mM $CaCl_2$, 2 mM $MgSO_4$, 26 mM $NaHCO_3$, 1.25 mM NaH_2PO_4, pH 7.4) supplemented with 10 mM D-glucose

(Sigma-Aldrich). The hippocampal hemispheres were isolated, and 200-μm-thick slices were prepared on an ice-cold McIllwain tissue chopper (Stoelting, Guildford, Surrey, UK). Slices from each hemisphere were transferred to freshly prepared, carbogen-bubbled aCSF supplemented with 10 mM D-glucose at 37°C for 1 h. The hippocampal slices were stimulated with 1 mM dibutyryl-cAMP for 15 min in aCSF supplemented with 0.1 mM D-glucose and 2 mM 2-deoxyglucose, following which 100 nM HFI-419 was added to slices from 1 hemisphere while the slices from the other hemisphere served as control. Then, 0.1 μCi 2-deoxy-D-[2, 6-³H]glucose (³H-2DG) (specific activity 49Ci/mmol; Amersham Biosciences, Rydalmere, NSW, Australia) was added to the slices for 5 min. Slices from the 2 hemispheres were then rinsed in 4 changes of ice-cold PBS, transferred to pre-weighed filter paper, dried, weighed, and solubilized overnight with Soluene-350 (Perkin Elmer, Wellesley, MA, USA). Tritium content was measured in a liquid scintillation analyser 1900TR (Perkin Elmer).

Statistical analysis

Statistical analyses were performed with GraphPad Prism (GraphPad Software Inc, San Diego, CA, USA) or SigmaStat (Systat Software, Chicago, IL, USA) software. Data are expressed as means ± SE and were analyzed with Student's t test (glucose uptake) or 1- or 2-way analysis of variance with Dunnett's *post hoc* analysis, where appropriate. A value of $P < 0.05$ was considered significant.

RESULTS

Molecular model of IRAP

In the absence of an experimentally determined structure of IRAP, a molecular model of the catalytic domain of IRAP was built based on the crystal structure of the related enzyme, LTA4H, bound to the metalloprotease inhibitor, bestatin (**Fig. 1**) (34). Analysis of models of the catalytic cleft of IRAP and LTA4H revealed an important difference, conferred by the amino acid residues L463 and A407 in IRAP, when compared to the corresponding amino acids F314 and Y267 in LTA4H (Fig. 1, insert). The smaller amino acid side-chains of IRAP alter the shape of its catalytic cleft when compared to LTA4H, and we predicted that the difference in these residues would allow the *in silico* identification of potential ligands that are selective with respect to the structural template LTA4H, used for building the IRAP model, LTA4H.

Virtual screening

An in-house database of 1.5 million compounds was screened against the homology model of IRAP, and 58 compounds with the highest docking scores were purchased and tested in the IRAP aminopeptidase assay. A hit rate of ~10% was achieved, with 6 structurally distinct compounds inhibiting the activity of IRAP with K_i values of ≤100 μM. HFI-14 (**Fig. 2A**) was selected for further development based on its relatively high affinity for IRAP and predicted drug-like properties. The binding of HFI-14 to the catalytic site of IRAP was proven by competitive enzyme kinetics and its specificity for IRAP was
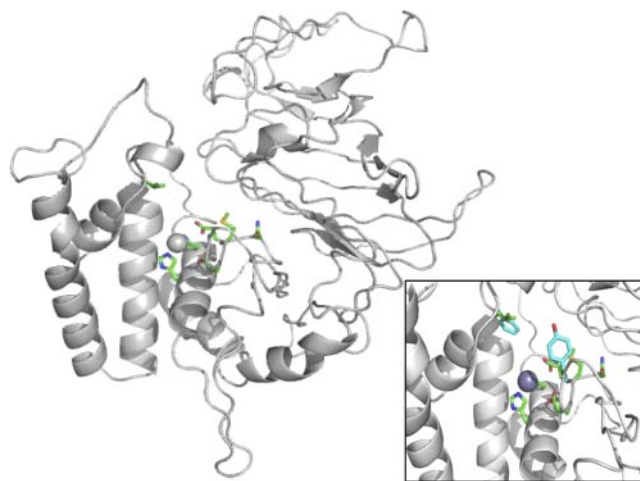

Figure 1. Homology model of the catalytic domain of IRAP. Diagrammatic representation of the homology model of IRAP used to identify inhibitors by virtual screening, with details of the catalytic site highlighting the differences between the model and LTA4H. The protein is shown in a cartoon representation with the active site residues shown as sticks colored by atom type, with carbon atoms shown in green. The zinc ion is shown as a gray sphere. Insert: Close-up view of the catalytic cleft of IRAP with the protein displayed as above. Residues F314 and Y267 of the template protein LTA4H are shown as sticks colored by atom type except carbon–carbon bonds, which are cyan. The two larger residues in LTA4H close off the top of the catalytic cleft, thereby making the pocket smaller than in IRAP.

confirmed by insignificant inhibitory effects on a range of enzymes including the related aminopeptidases, LTA4H and aminopeptidase N.

A sequential analog identification strategy was then employed, based on both shape and structural similarity to HFI-14, and a further 200 compounds were selected and assayed for IRAP inhibitory activity. In the first approach, we searched for compounds in our chemical database that had similar 3D shapes to HFI-14, but not necessarily the same core chemical structure. In the second approach, we searched for compounds with a similar core chemical structure. The outcome of secondary and subsequent screenings was the identification of structural homologs of HFI-14 with improved inhibitory activity. The most active compound, HFI-142, exhibited a K_i of 2 μM (Fig. 2B). Moreover, this screening approach identified a second family of structurally distinct inhibitors, albeit with lower activity (data not shown). Further development of the second family of IRAP inhibitors was not pursued at this time. The selectivity of the HFI-142 series for IRAP was tested experimentally and these compounds were found to exhibit limited inhibition of a range of related aminopeptidases and no inhibition of unrelated enzymes at concentrations of up to 100 μM (results not shown).

Medicinal chemistry modification

To facilitate a hit-to-lead transition, the potency of the inhibitors needed to be increased at least 1 order of magnitude relative to the original HFI-14 compound.
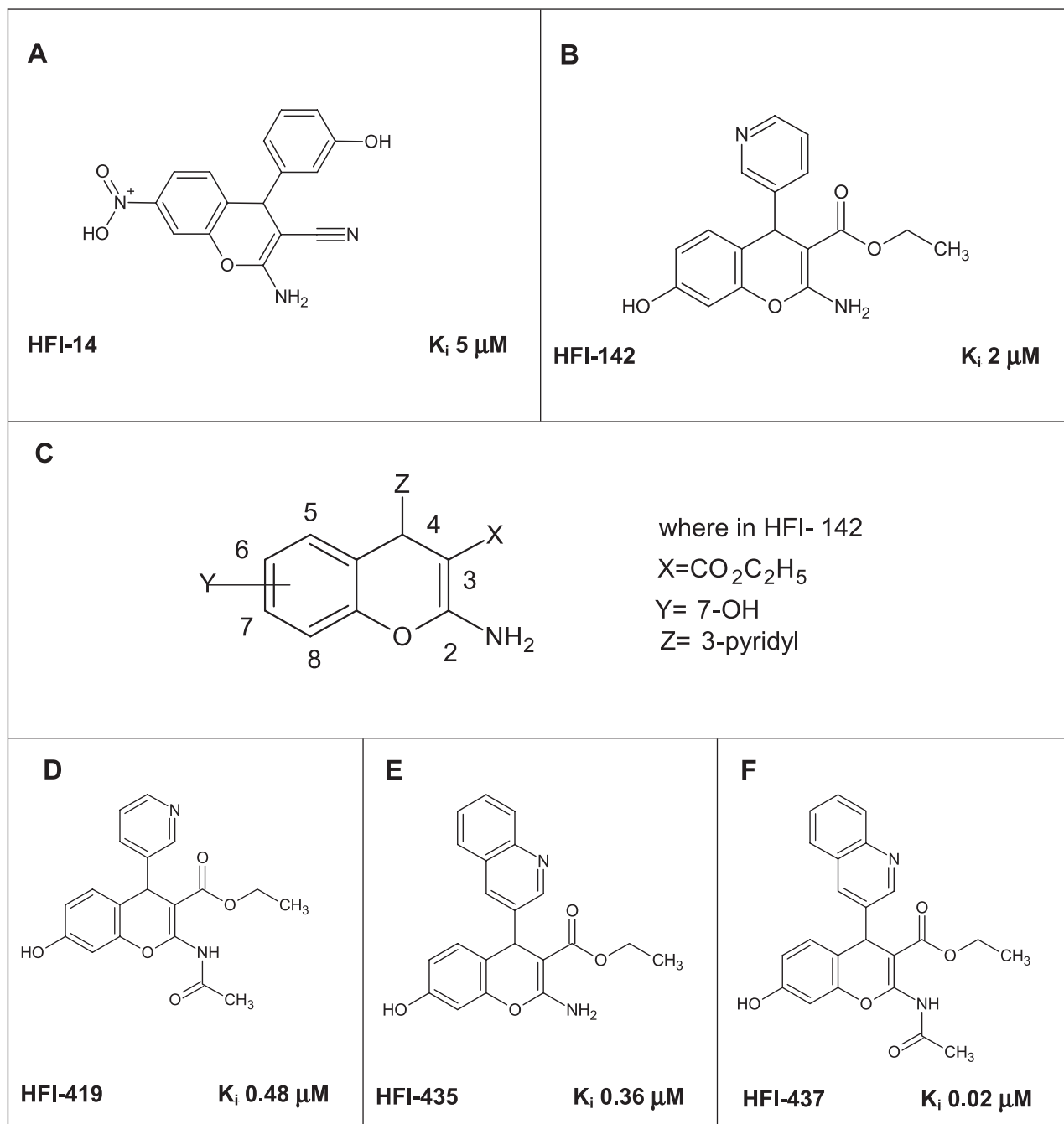
Figure 2. *A*) Structure of HFI-14 that was used for sequential shape- and structure-based screen of the compound library, leading to the identification of HFI-142 (*B*). *C*) Chemical modifications of the side-chains of HFI-142. *D–F*) Analogs with the highest affinity for IRAP, with K_i calculated for the synthetic substrate Leu-MCA, $K_i = IC_{50}/(1+[S]/K_m)$, where Leu-MCA $K_m = 38.7$ µM; [S] = 25 µM.

New derivatives with conservative modifications of the functional groups in HFI-142 [*i.e.*, the 2-amino, 7-hydroxy, ester, and 4-(3-pyridyl) groups] were synthesized (Fig. 2*C*). Thirty derivatives were purified and tested, with 12 structural analogs of HFI-142 displaying IRAP inhibitory activity.

Biochemical characterization of HFI-142 analogues

Three compounds, HFI-419 (ethyl 2-acetylamino-7-hydroxy-4-pyridin-3-yl-4H-chromene-3-carboxylate), made by acetylation of the 2-amino group of HFI-142; the quinoline analog HFI-435; and the hybrid molecule HFI-437 (ethyl 2-acetylamino-7-hydroxy-4-quinolin-3-yl-4H-chromene-3-carboxylate) exhibited K_i values of <1 µM (Fig. 2*D–F*). The compound with the highest activity, HFI-437, exhibited a K_i value of 20 nM, 250-fold higher than the original hit compound, HFI-14. The specificity of the HFI-142 analogs for IRAP was confirmed experimentally: The compounds exhibited much lower affinities (>1000-fold lower) for the structurally related enzymes, endoplasmic reticulum-

associated aminopeptidase 1 and 2, aminopeptidase N, and, more important, LTA4H (**Table 1**). Unlike angiotensin IV, these compounds (at 100 μM) were completely inactive in competing for angiotensin II binding to the AT_1 receptor (results not shown).

The physicochemical characteristics of HFI-142, HFI-419, HFI-435, and HFI-437 were evaluated by both *in silico* and experimental techniques. Solubility was assessed at pH 2.0 and 6.5 by turbidimetric assay. Under acidic conditions, all compounds display good solubility (>100 μg/ml). At pH 6.5, HFI-142 and HFI-419 displayed moderate and similar solubility values, 25–50 and 50–100 μg/ml, respectively. Solubility values for HFI-435 and HFI-437 were significantly lower, at 3–6 and 6–12 μg/ml, respectively.

The brain uptake of the 4 compounds in this series was low. Five minutes after an i.v. dose of 5 mg/kg, the mean brain-to-plasma (B:P) ratios were 0.24, 0.39, 0.20, and 0.11 for HFI-142, HFI-419, HFI-435, and HFI-437, respectively. At 60 min postdose, the mean B:P ratios for HFI-142 and HFI-435 were 0.22 and 0.52, respectively. Brain concentrations of HFI-419 and HFI-437 were not detected at 60 min postdose. Following i.v. infusion of HFI-419 and HFI-437, concentrations of HFI-142 and HFI-435, respectively, were detected, suggesting hydrolysis of the amide moiety had occurred *in vivo*.

Effects of HFI-419 in the central nervous system

To evaluate the central effects of these IRAP inhibitors, HFI-419 was selected on the basis of its relatively high affinity for IRAP and its solubility profile. Initially, the effect of HFI-419 was tested *in vitro* in a hippocampal slice assay to investigate whether the drug modulated glucose uptake. Consistent with the effect of peptide inhibitors of IRAP, HFI-419 at a concentration of 100 nM significantly increased dibutyryl cAMP-evoked glucose uptake in rat hippocampal slices ($t=2.81$, $P<0.05$) (**Fig. 3**).

The effects of centrally administered HFI-419 on 2 distinct memory tasks were then investigated in rats. In the novel object recognition task, there was a significant treatment effect ($F_{(2,27)}=8.02$, $P<0.05$) with rats treated with 0.1 or 1 nmol HFI-419 5 min prior to the acquisi-
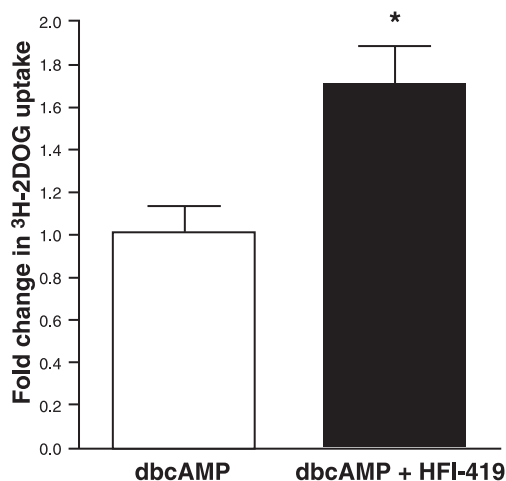
Figure 3. Effect of HFI-419 in an *in vitro* bioassay: determination of glucose uptake in rat hippocampal slices. HFI-419 significantly enhanced dbcAMP-stimulated (^{3}H-2DG) glucose uptake in rat hippocampal slices ($n=7$/group; $P<0.05$).

tion trial spending significantly more time investigating the novel object than the familiar object following an intertrial interval of 20 h ($P<0.05$ and $P<0.01$, respectively). At this intertrial interval, control vehicle-treated rats did not discriminate between the familiar and the novel object, with recognition indices that did not differ significantly from chance performance (**Fig. 4A**).

In the spontaneous alternation plus maze task, a significant treatment effect was detected in the alternation score ($F_{(2,21)}=6.18$, $P<0.01$), with rats that received the dose of 0.1 nmol HFI-419 5 min prior to testing obtaining significantly higher alternation scores compared to control vehicle-treated rats ($P<0.01$), demonstrating enhanced spatial working memory (Fig. 4B). In contrast, in the measurement of the number of arm entries, no significant treatment effect was detected ($F_{(2,21)}=0.90$, $P>0.05$), indicating that the drug treatment did not alter the rate or speed of movement in the maze.

Since performance of the rats in the memory paradigms is dependent on their motor ability and state of mind, the effect of the HFI-419 on locomotor activity and anxiety levels was also tested in rats after central adminis-

TABLE 1. *Percentage inhibition of related and unrelated enzymes*

Enzyme	HFI-419		HFI-435		HFI-437	
	100 μM	10 μM	100 μM	10 μM	100 μM	10 μM
Glucose-6-phosphate (EC 1.1.1.49) dehydrogenase/ glucose hexokinase (EC 2.7.1.1)	0	ND	0	ND	0	ND
Leukotriene A4 hydrolase (EC 3.3.2.6)	0	ND	4	ND	25	0
Aminopeptidase N (EC 3.4.11.2)	6	12	2	10	1	1
Endoplasmic reticulum-associated aminopeptidase 1 (EC 3.4.11.22)	5	0	12	3	7	0
Endoplasmic reticulum-associated aminopeptidase 2 (EC 3.4.11)	13	2	21	6	18	4
Angiotensin-converting enzyme 1 (EC 3.4.15.1)	3	9	3	0	0	0

Determination of the inhibitory activity of the HFI-142 analogs for other enzymes. Results are expressed as percentage inhibition of the catalytic activity of the enzyme at the given concentration; $n = 3–4$. ND, not determined.
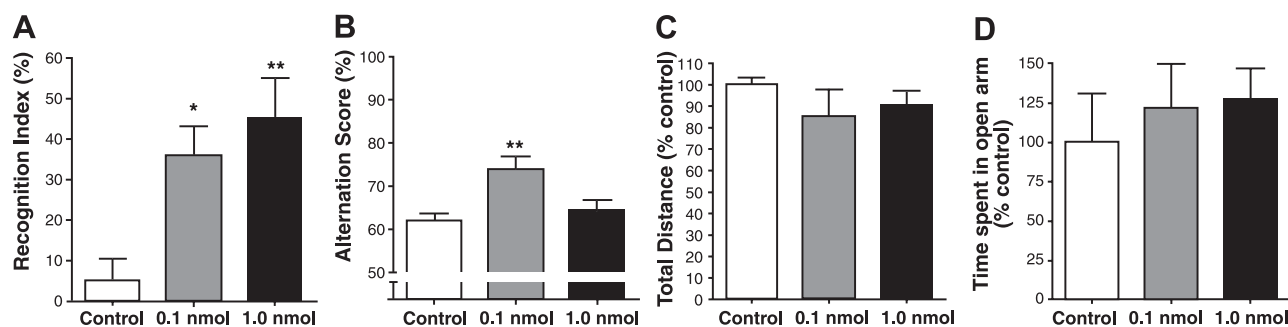
Figure 4. Effect of HFI-419 in *in vivo* bioassays. *A*) Rats treated with HFI-419 at 1 and 0.1 nmol intracerebroventricularly (i.c.v.) exhibited better recognition of a novel object after 20 h compared to vehicle treated control rats (*n*=9–11/group). *B*) Rats treated with 0.1 nmol HFI-419 exhibited significantly enhanced spontaneous alternation scores compared to vehicle treated control rats (*n*=8/group). *C*) Rats treated with HFI-419 at 0.1 and 1 nmol i.c.v. did not exhibit different locomotor activity compared to vehicle treated rats, as determined by crossing of infrared beams and total distance traveled in a locomotor cell (*n*=5–8/ group). *D*) Rats treated with HFI-419 at 0.1 and 1 nmol i.c.v. did not demonstrate altered levels of anxiety compared to vehicle-treated control rats, as determined by time spent in the open arm of the elevated plus maze (*n*=5–8/group). *$P <$ 0.05; **$P < 0.01$.

tration. Rats treated with the doses of HFI-419 that elicited the memory effects displayed the same level of activity as the vehicle-treated controls, as determined by crossing of infrared beams in a locomotor cell over a period of 30 min ($F_{(2,21)}$=0.80, $P>0.05$) (Fig. 4C). The same doses of HFI-419 did not significantly alter the time spent in the open arms in the elevated plus maze ($F_{(2,22)}$=0.60, $P>0.05$), which is a measure of anxiety (Fig. 4D). Therefore, IRAP inhibition by HFI-419 selectively affects central mechanisms involved in memory processing, resulting in improved performance in memory tasks without impacting on locomotor activity or anxiety, factors that can influence the outcome of the memory tasks.

DISCUSSION

Effects of peptide inhibitors of IRAP in the central nervous system

The peptides Ang IV (VYIHPF) and LVV-H7 (LVVYP-WTQRF) exhibit very similar effects in the central nervous system, potentiating potassium-evoked acetyl-choline release (40) and glucose uptake (21) from hippocampal slices, accelerating spatial learning in rats after a single acute dose (5) and ameliorating memory deficits induced by the muscarinic receptor antagonist, scopolamine (8, 9, 11). In support of a role for Ang IV in memory processing, the hexapeptide was found to enhance long-term potentiation in the hippocampus *in vitro* (41) and *in vivo* (42).

Both peptides bind with high affinity to IRAP (19) and are competitive inhibitors of the enzyme, but are not substrates (15). In view of the biochemical and pharmacological properties of the 2 peptides, it is proposed that IRAP is involved in mediating their memory-enhancing effects. Consistent with this proposal, IRAP is abundantly expressed in neurons in the basal forebrain, amygdale, hippocampus, and entorhi-

nal cortex (20, 43, 44), brain regions that are integrally involved in memory processing.

However, there is a level of promiscuity in these peptide IRAP inhibitors—at higher concentrations, Ang IV is capable of activating the angiotensin AT_1 receptor (45) and LVV-H7 the mu opioid receptor (46). In addition, both peptides also interact with aminopeptidase N, albeit at significantly higher concentrations than to IRAP (29, 30).

Provision of proof-of-concept that inhibition of IRAP results in facilitation of memory

The concept that IRAP is the central target of the memory enhancing peptides Ang IV and LVV-H7 has been controversial, with different groups proposing other targets for these peptides (31). Therefore, the *in silico* identification of specific inhibitors of IRAP based on their binding to the catalytic domain of this enzyme taken through to the demonstration of memory enhancing effects *in vivo* provides substantial proof of this concept. The newly identified and characterized IRAP inhibitor, HFI-419, when administered into the cerebral ventricles of rats, dose-dependently improved visual recognition memory as assessed by the novel object recognition task. Moreover, central administration of a single acute dose of HFI-419 also improved spatial working memory, as determined by increased spontaneous alternation in the plus maze. IRAP inhibitors are therefore able to enhance different forms of memory that involve distinct brain circuitries (47, 48).

The demonstration that HFI-419 enhances glucose uptake in the hippocampal slices provides a potentially important mechanism of action and is supported by previous observations of an identical effect elicited by the peptide inhibitors of IRAP (21). Our working hypothesis is that in neurons where IRAP and GLUT4 are colocalized, the IRAP inhibitors extend the half-life of IRAP and GLUT4 at the plasma membrane by altering the trafficking of these two proteins. The increased levels of IRAP

and GLUT4 on the cell surface result in more glucose being taken up by the neurons (21). Exogenous glucose administration has been shown to facilitate memory in rodents (49, 50) and to reverse memory deficits in animals (51, 52) and in humans (22, 50).

Novelty and effectiveness of screening strategy

In addition to hit identification through virtual screening, the computational iterative drug refinement strategy adopted in this study provided a valuable and cost-effective approach to support lead optimization efforts (32). From a single compound identified in the first round of screening, 2 distinct classes of small molecular weight IRAP inhibitors emerged, following consecutive rounds of either 3D shape-based or core structure-based sequential screens, with successful "hit" rates of between 6–10%. Minor conservative modification of a functional group of the highest affinity compound identified by virtual screening resulted in a 5-fold improvement in affinity and demonstrated efficacy in biological assays, including 2 *in vivo* tests of memory function.

The previous reported success of the utility of homology models in virtual screening was predominantly in *in silico* ligand design, where the models were employed to identify novel compounds based on the structure of known ligands (32, 53). However, in the less common cases where the homology models were used for high throughput *in silico* screening for compounds for new targets, the majority of the models were based on crystal structures of proteins with high sequence homology with the targets. This often resulted in the identification of compounds that also interacted with high affinity with the protein on which the model was based (32, 53). In contrast, IRAP and LTA4H share only 41% sequence identity across the catalytic domain, including distinct differences enabling the identification of inhibitors of IRAP that did not bind to LTA4H.

CONCLUSIONS

Our successful development of a potent, selective, and centrally active class of IRAP inhibitors validates the enzyme as a promising target for therapeutic strategies directed toward cognitive disorders. The small-molecule inhibitors of IRAP identified in this study will also provide valuable pharmacological tools for delineating the physiological roles of the enzyme. This body of work also highlights the value of computational drug discovery, not only in accelerating the identification of hit compounds but also in their development into lead series. [FJ]

REFERENCES

1. Furey, M. L., Pietrini, P., and Haxby, J. V. (2000) Cholinergic enhancement and increased selectivity of perceptual processing during working memory. *Science* **290,** 2315–2319
2. Braszko, J. J., Kupryszewski, G., Witczuk, B., and Wisniewski, K. (1988) Angiotensin II-(3–8)-hexapeptide affects motor activity, performance of passive avoidance and a conditioned avoidance response in rats. *Neuroscience* **27,** 777–783
3. Wright, J. W., Miller-Wing, A. V., Shaffer, M. J., Higginson, C., Wright, D. E., Hanesworth, J. M., and Harding, J. W. (1993) Angiotensin II(3–8) (ANG IV) hippocampal binding: potential role in the facilitation of memory. *Brain Res. Bull.* **32,** 497–502
4. Wright, J. W., Stubley, L., Pederson, E. S., Kramar, E. A., Hanesworth, J. M., and Harding, J. W. (1999) Contributions of the brain angiotensin IV-AT4 receptor subtype system to spatial learning. *J. Neurosci.* **19,** 3952–3961
5. Lee, J., Albiston, A. L., Allen, A. M., Mendelsohn, F. A. O., Ping, S. E., Barrett, G. L., Murphy, M., Morris, M. J., McDowall, S. G., and Chai, S. Y. (2004) Effect of intracerebroventricular injection of AT4 receptor ligands, Nle1-angiotensin IV and LVv-hemorphin 7, on spatial learning in rats. *Neuroscience* **124,** 341–349
6. Wisniewski, K., Borawska, M., and Car, H. (1993) The effect of angiotensin II and its fragments on post-alcohol impairment of learning and memory. *Pol. J. Pharmacol.* **45,** 23–29
7. Wright, J. W., Clemens, J. A., Panetta, J. A., Smalstig, E. B., Weatherly, L. A., Kramar, E. A., Pederson, E. S., Mungall, B. H., and Harding, J. W. (1996) Effects of LY231617 and angiotensin IV on ischemia-induced deficits in circular water maze and passive avoidance performance in rats. *Brain Res.* **717,** 1–11
8. Pederson, E. S., Harding, J. W., and Wright, J. W. (1998) Attenuation of scopolamine-induced spatial learning impairments by an angiotensin IV analog. *Regul. Pept.* **74,** 97–103
9. Pederson, E. S., Krishnan, R., Harding, J. W., and Wright, J. W. (2001) A role for the angiotensin AT4 receptor subtype in overcoming scopolamine-induced spatial memory deficits. *Regul. Pept.* **102,** 147–156
10. Olson, M. L., Olson, E. A., Qualls, J. H., Stratton, J. J., Harding, J. W., and Wright, J. W. (2004) Norleucine1-angiotensin IV alleviates mecamylamine-induced spatial memory deficits. *Peptides* **25,** 233–241
11. Albiston, A. L., Pederson, E. S., Burns, P., Purcell, B., Wright, J. W., Harding, J. W., Mendelsohn, F. A., Weisinger, R. S., and Chai, S. Y. (2004) Reversal of scopolamine-induced memory deficits by LVV-hemorphin 7 in rats in the passive avoidance and Morris water maze paradigms. *Behav. Brain Res.* **154,** 239–243
12. Chai, S. Y., Fernando, R., Peck, G., Ye, S. Y., Mendelsohn, F. A. O., Jenkins, T. A., and Albiston, A. L. (2004) The angiotensin IV/AT4 receptor. *Cell Mol. Life Sci.* **61,** 2728–2737
13. Albiston, A. L., Mustafa, T., McDowall, S. G., Mendelsohn, F. A., Lee, J., and Chai, S. Y. (2003) AT(4) receptor is insulin-regulated membrane aminopeptidase: potential mechanisms of memory enhancement. *Trends Endocrinol. Metab.* **14,** 72–77
14. Herbst, J. J., Ross, S. A., Scott, H. M., Bobin, S. A., Morris, N. J., Lienhard, G. E., and Keller, S. R. (1997) Insulin stimulates cell surface aminopeptidase activity toward vasopressin in adipocytes. *Am. J. Physiol.* **272,** E600–606
15. Lew, R. A., Mustafa, T., Ye, S., McDowall, S. G., Chai, S. Y., and Albiston, A. L. (2003) Angiotensin AT4 ligands are potent, competitive inhibitors of insulin regulated aminopeptidase (IRAP). *J. Neurochem.* **86,** 344–350
16. Keller, S. R., Scott, H. M., Mastick, C. C., Aebersold, R., and Lienhard, G. E. (1995) Cloning and characterization of a novel

insulin-regulated membrane aminopeptidase from Glut4 vesicles. *J. Biol. Chem.* **270,** 23612–23618

17. Waters, S. B., D'Auria, M., Martin, S. S., Nguyen, C., Kozma, L. M., and Luskey, K. L. (1997) The amino terminus of insulin-responsive aminopeptidase causes Glut4 translocation in 3T3-L1 adipocytes. *J. Biol. Chem.* **272,** 23323–23327

18. Rogi, T., Tsujimoto, M., Nakazato, H., Mizutani, S., and Tomoda, Y. (1996) Human placental leucine aminopeptidase/oxytocinase. A new member of type II membrane-spanning zinc metallopeptidase family. *J. Biol. Chem.* **271,** 56–61

19. Albiston, A. L., McDowall, S. G., Matsacos, D., Sim, P., Clune, E., Mustafa, T., Lee, J., Mendelsohn, F. A., Simpson, R. J., Connolly, L. M., and Chai, S. Y. (2001) Evidence that the angiotensin IV (AT4) receptor is the enzyme insulin regulated aminopeptidase. *J. Biol. Chem.* **276,** 48263–48266

20. Fernando, R., Larm, J., Albiston, A. L., and Chai, S. Y. (2005) Distribution and cellular localization of the insulin regulated aminopeptidase (IRAP) in the rat central nervous system. *J. Comp. Neurol.* **487,** 372–390

21. Fernando, R., Albiston, A. L., and Chai, S. Y. (2008) The insulin-regulated aminopeptidase IRAP is co-localised with GLUT4 in the mouse hippocampus – potential role in modulation of glucose uptake in neurones? *Eur. J. Neurosci.* **28,** 588–598.

22. Korol, D. L., and Gold, P. E. (1998) Glucose, memory, and aging. *Am. J. Clin. Nutr.* **67,** 764S–771S

23. Manning, C. A., Ragozzino, M. E., and Gold, P. E. (1993) Glucose enhancement of memory in patients with probable senile dementia of the Alzheimer's type. *Neurobiol. Aging* **14,** 523–528

24. Dash, P. K., Orsi, S. A., and Moore, A. N. (2006) Spatial memory formation and memory-enhancing effect of glucose involves activation of the tuberous sclerosis complex-mammalian target of rapamycin pathway. *J. Neurosci.* **26,** 8048–8056

25. McNay, E. C., Fries, T. M., and Gold, P. E. (2000) Decreases in rat extracellular hippocampal glucose concentration associated with cognitive demand during a spatial task. *Proc. Natl. Acad. Sci. U. S. A.* **97,** 2881–2885

26. Kobori, T., Goda, K., Sugimoto, K., Ota, T., and Tomisawa, K. (1995) Amino compounds and angiotensin IV receptor agonists. U.S. patent 6,066,672, issued May 23, 2000

27. Albiston, A. L., Peck, G. R., Yeatman, H. R., Fernando, R., Ye, S., and Chai, S. Y. (2007) Therapeutic targeting of insulin-regulated aminopeptidase: heads and tails? *Pharmacol. Ther.* **116,** 417–427

28. Axen, A., Lindeberg, G., Demaegdt, H., Vauquelin, G., Karlen, A., and Hallberg, M. (2006) Cyclic insulin-regulated aminopeptidase (IRAP)/AT4 receptor ligands. *J. Pept. Sci.* **12,** 705–713

29. Garreau, I., Chansel, D., Vandermeersch, S., Fruitier, I., Piot, J. M., and Ardaillou, R. (1998) Hemorphins inhibit angiotensin IV binding and interact with aminopeptidase N. *Peptides* **19,** 1339–1348

30. Demaegdt, H., Lenaerts, P. J., Swales, J., De Backer, J. P., Laeremans, H., Le, M. T., Kersemans, K., Vogel, L. K., Michotte, Y., Vanderheyden, P., and Vauquelin, G. (2006) Angiotensin AT4 receptor ligand interaction with cystinyl aminopeptidase and aminopeptidase N: [125I]angiotensin IV only binds to the cystinyl aminopeptidase apo-enzyme. *Eur. J. Pharmacol.* **546,** 19–27

31. Wright, J. W., Yamamoto, B. J., and Harding, J. W. (2008) Angiotensin receptor subtype mediated physiologies and behaviors: new discoveries and clinical targets. *Prog. Neurobiol.* **84,** 157–181

32. Kitchen, D. B., Decornez, H., Furr, J. R., and Bajorath, J. (2004) Docking and scoring in virtual screening for drug discovery: methods and applications. *Nat. Rev. Drug Discov.* **3,** 935–949

33. Loging, W., Harland, L., and Williams-Jones, B. (2007) High-throughput electronic biology: mining information for drug discovery. *Nat. Rev. Drug Discov.* **6,** 220–230

34. Thunnissen, M. M., Nordlund, P., and Haeggstrom, J. Z. (2001) Crystal structure of human leukotriene A(4) hydrolase, a bifunctional enzyme in inflammation. *Nat. Struct. Biol.* **8,** 131–135

35. Eisenberg, D., Luthy, R., and Bowie, J. U. (1997) VERIFY3D: assessment of protein models with three-dimensional profiles. *Methods Enzymol.* **277,** 396–404

36. Al-Mousawi, S. M., Elkholy, Y. M., Mohammad, M. A., and Elnagdi, M. H. (1999) Synthesis of new condensed 2-amino-4H-pyran-3-carbonitriles and of 2-aminoquinoline-3-carbonitriles. *Org. Preparations Proced. Int.* **31,** 305–313

37. Paxinos, G., and Watson, C. (1986) *The Rat Brain in Stereotaxic Coordinates,* Academic Press, San Diego, CA, USA

38. Bevins, R. A., and Besheer, J. (2006) Object recognition in rats and mice: a one-trial non-matching-to-sample learning task to study 'recognition memory.' *Nat. Protoc.* **1,** 1306–1311

39. Diano, S., Farr, S. A., Benoit, S. C., McNay, E. C., da Silva, I., Horvath, B., Gaskin, F. S., Nonaka, N., Jaeger, L. B., Banks, W. A., Morley, J. E., Pinto, S., Sherwin, R. S., Xu, L., Yamada, K. A., Sleeman, M. W., Tschop, M. H., and Horvath, T. L. (2006) Ghrelin controls hippocampal spine synapse density and memory performance. *Nat. Neurosci.* **9,** 381–388

40. Lee, J., Chai, S. Y., Mendelsohn, F. A., Morris, M. J., and Allen, A. M. (2001) Potentiation of cholinergic transmission in the rat hippocampus by angiotensin IV and LVV-hemorphin-7. *Neuropharmacology* **40,** 618–623

41. Kramar, E. A., Armstrong, D. L., Ikeda, S., Wayner, M. J., Harding, J. W., and Wright, J. W. (2001) The effects of angiotensin IV analogs on long-term potentiation within the CA1 region of the hippocampus in vitro. *Brain Res.* **897,** 114–121

42. Wayner, M. J., Armstrong, D. L., Phelix, C. F., Wright, J. W., and Harding, J. W. (2001) Angiotensin IV enhances LTP in rat dentate gyrus in vivo. *Peptides* **22,** 1403–1414

43. Moeller, I., Paxinos, G., Mendelsohn, F. A., Aldred, G. P., Casley, D., and Chai, S. Y. (1996) Distribution of AT4 receptors in the *Macaca fascicularis* brain. *Brain Res.* **712,** 307–324

44. Chai, S. Y., Bastias, M. A., Clune, E. F., Matsacos, D. J., Mustafa, T., Lee, J. H., McDowall, S. G., Mendelsohn, F. A., Paxinos, G., and Albiston, A. L. (2000) Distribution of angiotensin IV binding sites (AT(4) receptor) in the human forebrain, midbrain and pons as visualised by in vitro receptor autoradiography. *J. Chem. Neuroanat.* **20,** 339–348

45. Wright, J. W., Bechtholt, A. J., Chambers, S. L., and Harding, J. W. (1996) Angiotensin III and IV activation of the brain AT1 receptor subtype in cardiovascular function. *Peptides* **17,** 1365–1371

46. Nyberg, G., Sanderson, K., Andren, P., Thornwall, M., Einarsson, M., Danielson, B., and Nyberg, F. (1996) Isolation of haemorphin-related peptides from filter membranes collected in connection with haemofiltration of human subjects. *J. Chromatogr. A* **723,** 43–49

47. Funahashi, S. (2006) Prefrontal cortex and working memory processes. *Neuroscience* **139,** 251–261

48. Kesner, R. P., Ravindranathan, A., Jackson, P., Giles, R., and Chiba, A. A. (2001) A neural circuit analysis of visual recognition memory: role of perirhinal, medial, and lateral entorhinal cortex. *Learn. Mem.* **8,** 87–95

49. Lee, M. K., Graham, S. N., and Gold, P. E. (1988) Memory-enhancement with post-training intraventricular glucose injections in rats. *Behav. Neurosci.* **102,** 591–595

50. Ragozzino, M. E., Pal, S. N., Unick, K., Stefani, M. R., and Gold, P. E. (1998) Modulation of hippocampal acetylcholine release and spontaneous alternation scores by intrahippocampal glucose injections. *J. Neurosci.* **18,** 1595–1601

51. Parkes, M., and White, K. G. (2000) Glucose attenuation of memory impairments. *Behav. Neurosci.* **114,** 307–319

52. Parent, M. B., Laurey, P. T., Wilkniss, S., and Gold, P. E. (1997) Intraseptal infusions of muscimol impair spontaneous alternation performance: infusions of glucose into the hippocampus, but not the medial septum, reverse the deficit. *Neurobiol. Learn. Mem.* **68,** 75–85

53. Hillisch, A., Pineda, L. F., and Hilgenfeld, R. (2004) Utility of homology models in the drug discovery process. *Drug Discov. Today* **9,** 659–669